PHYSICAL REVIEW C VOLUME 23, NUMBER 2 FEBRUARY 1981

Charged-particle emission in reactions of 15-MeV neutrons with ^{89}Y, ^{90}Zr, and ^{92,94,95,96}Mo

R. C. Haight, S. M. Grimes, and R. G. Johnson*
Lawrence Livermore National Laboratory, Livermore, California 94550

H. H. Barschall
University of Wisconsin, Madison, Wisconsin 53706
(Received 17 October 1980)

Charged-particle emission cross sections, spectra, and angular distributions have been measured for targets of ^{89}Y, ^{90}Zr, and ^{92,94,95,96}Mo bombarded with 14.8-MeV neutrons. A magnetic quadrupole spectrometer served to detect the charged particles. Evidence for both statistical and pre-equilibrium reaction mechanisms was found in the proton, deuteron, and alpha-particle emission. The cross sections and spectra are compared with calculations based on these reaction models.

[NUCLEAR REACTIONS ^{89}Y, ^{90}Zr, ^{92,94,95,96}Mo. (n,p), (n,d), (n,α), $E=14.8$ MeV; measured $\sigma(E_p,\theta)$, $\sigma(E_d,\theta)$, $\sigma(E_\alpha,\theta)$, enriched targets. Hauser-Feshbach and hybrid pre-equilibrium analysis, deduced reaction mechanisms.]

I. INTRODUCTION

Measurements of cross sections for the emission of protons, deuterons, and α particles in reactions of 15-MeV neutrons with intermediate weight nuclides have been reported in previous papers.[1-3] Nuclides that have been investigated ranged from ^{27}Al to ^{93}Nb with special attention to the isotopes of Cr, Fe, Ni, and Cu. These measurements have shown wide variations between isotopes. For example, the proton-emission cross section of ^{54}Fe is almost five times that of ^{56}Fe, and the α-particle emission cross section of ^{63}Cu is about four times that of ^{65}Cu. Analysis of the data in terms of statistical and pre-equilibrium models could account for most of the observations, not only of the total emission cross section but also of the energy spectra.

The present measurements extend our studies in the mass-90 region. Together with the previous study of ^{93}Nb, these measurements provide data to test nuclear reaction models in this region of both proton and neutron closed shells.

A knowledge of these emission cross sections is also important for assessing radiation damage in fusion reactors. Zirconium and molybdenum have been proposed as constituents of structural materials for fusion reactors, so that the measurements are of interest for this application.

II. EXPERIMENTAL PROCEDURE

The charged-particle-emission cross sections were measured by detecting protons, deuterons, and alpha particles with a magnetic quadrupole spectrometer.[4] The operation of this spectrometer has been described in Ref. 1. The spectrometer consists of a magnetic quadrupole triplet lens system that transports the charged particles, and ΔE-E silicon surface-barrier detectors that identify the particles and determine their energy.

The circular target foils, 2.5 cm in diameter, were made of rolled metals.[5] Their thicknesses and principal isotopic components are given in Table I. Target thicknesses were determined by measuring the energy loss of 5.48-MeV alpha particles. Variations in thickness were less than 5%, which is negligible for the present measurements. Average thicknesses determined by weighing agreed with those from the energy-loss measurements within 6%. To indicate the limit of resolution in the measurements, the energy loss in half the foil thickness is given in Table I for typical particles (5-MeV protons, 12-MeV alpha particles).

The source-to-target distances, the variation of neutron energy with angle (14.4 to 15.2 MeV), and the angular range subtended in these measurements ($\pm 7°$) were nearly the same as those given in Table II of Ref. 1. The only significant difference is that in the present measurements at 80° and 90° the center of the foil was 6.1 and 6.0 cm, respectively, from the center of the neutron source. This change was made to reduce the error in calculating the flux at the target foil.

Energy spectra were taken at several angles: for ^{89}Y at 25, 38, 80, and 128°, with partial spectra at 30, 45, 90, and 135°; for ^{90}Zr at 25, 38, 80, and 128°, with a partial spectrum at 90°; for ^{92}Mo at 25, 38, 80, and 128°, and partial spectra at 45, 90, and 135°; and for ^{94,95,96}Mo at 25, 45, 90, and 135°.

TABLE I. Target foils and composition.

Target foil	Thickness (mg/cm^2)	Principal isotopic constituents A (%)	Energy loss in half thickness of foil (MeV) 5-MeV proton	12-MeV alpha particle
^{89}Y	5.62	89(100)	0.11	0.61
^{90}Zr	5.94	90(97.65), 91(0.96), 92(0.71) 94(0.55), 96(0.13)	0.11	0.64
^{92}Mo	2.53	92(98.27), 94(0.46), 95(0.37) 96(0.26), 97(0.13), 98(0.27), 100(0.25)	0.05	0.27
^{94}Mo	2.63	92(0.87), 94(93.9), 95(2.85), 96(1.04) 97(0.40), 98(0.75), 100(0.22)	0.05	0.28
^{95}Mo	2.50	92(0.28), 94(0.58), 95(96.8), 96(1.54) 97(0.36), 98(0.45), 100(< 0.1)	0.05	0.26
^{96}Mo	2.54	92(0.18), 94(0.18), 95(0.94), 96(96.8) 97(0.96), 98(0.82), 100(0.1)	0.05	0.27

Contaminants in the proton spectra consisted of ^{1}H(n, p) recoil protons which were emitted from all targets at angles below 45° except for ^{90}Zr. The alpha-particle spectra contained products from ^{16}O(n, α) reactions which were identified by the variation of alpha-particle energy with emission angle. Because of the uncertainty in the corrections for these contaminants, we did not include the contaminated regions of the spectra in the analysis.

Two representative spectra are shown in Fig. 1 for 14.8-MeV neutron interactions: (a) protons from ^{92}Mo and (b) alpha particles from ^{94}Mo. The former interaction has the largest cross section measured in this study, and the latter is representative of a small cross section.

III. RESULTS

Differential energy spectra were measured in 500-keV bins and integrated over angle. The cross sections integrated over angle are shown in Figs. 2–4. Integration over energy yielded the total emission cross sections for protons, deuterons, and alpha particles listed in Table II. In addition, the average energies of the charged particles are given in Table II.

The systematic errors are nearly the same as those described in Ref. 1. The overall errors were 12% for protons, 15% for alpha particles, and 30% for deuterons. The distortion of the spectra due to energy loss in the target foil is somewhat less in this experiment than in our previous experiment because of the smaller energy loss in the targets, especially for the molybdenum isotopes, where thinner foils were used.

The angular distributions of the spectra were analyzed by Legendre polynomial expansions $\sigma(\theta) = \sum_{i=0}^{n} a_i P_i(\cos\theta)$. The a_0 coefficients determined the angle-integrated spectra of Figs. 2–4. Nearly all the proton and alpha-particle angular distributions could be fitted by setting $n = 2$. The

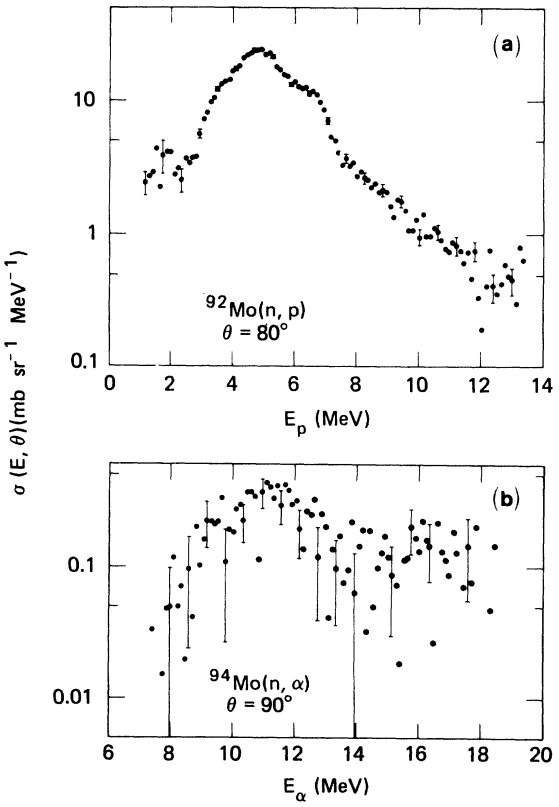

FIG. 1. Representative charged-particle emission spectra from targets bombarded by 14.8-MeV neutrons: (a) proton emission at 80° from ^{92}Mo; (b) alpha-particle emission at 90° from ^{94}Mo. Typical errors from counting statistics are shown.

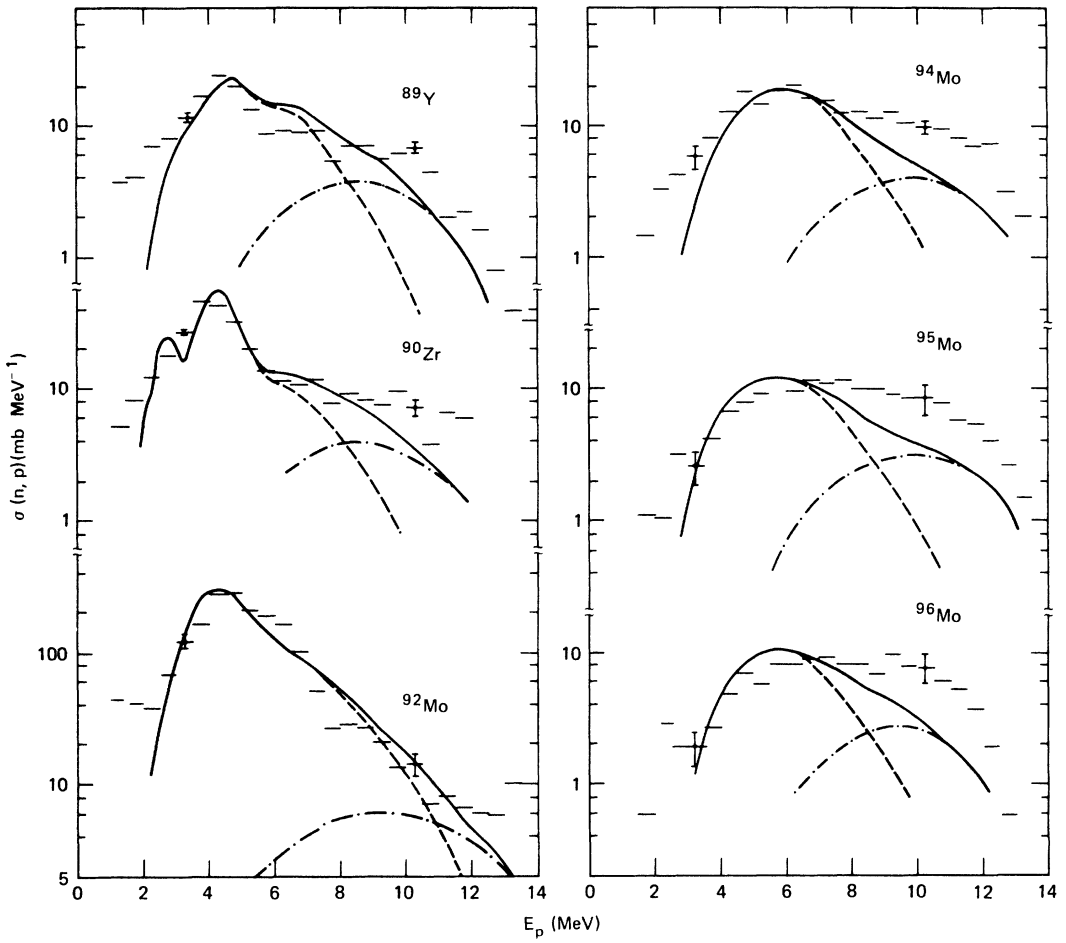

FIG. 2. Angle-integrated proton-emission cross sections for reactions induced by 14.8-MeV neutrons on targets of ^{89}Y, ^{90}Zr, and ^{92,94,95,96}Mo. The horizontal bars denote the experimental values in 500 keV bins. Typical statistical errors are shown. The multistage Hauser-Feshbach calculation is represented by the dashed line. The hybrid-model calculation for pre-equilibrium emission is denoted by the dot-dashed line. The sum of the two calculations is given by the solid line.

ratios of the resulting coefficients a_1/a_0 and a_2/a_0 are given in Figs. 5 and 6 as a function of emission energy for protons and alpha particles. The variations between neighboring points indicate the uncertainties in these ratios. At the high and low ends of the spectra where the cross sections are small, the counting statistics are poor and the fluctuations are largest.

A systematic error in these ratios could be caused by an error in the angular calibration. Angles are changed by translational motion of the spectrometer relative to the neutron source (see Ref. 1). An error in the translational position may be the cause of the negative values of a_1/a_0 for ^{94,95,96}Mo in regions where we expect the emission cross section to be symmetric about 90°, i.e., for 5–7-MeV protons and for 8–11-MeV alpha particles. These isotopes were investigated together, and separately from ^{89}Y, ^{90}Zr, and ^{92}Mo. A slight increase in a_1/a_0 would produce the expected symmetry.

Charged-particle emission cross sections for natural molybdenum were deduced from the isotopic data using estimates for the unmeasured isotopes ^{97,98,100}Mo. The average values chosen for ^{97,98,100}Mo for proton-, deuteron-, and alpha-particle-emission cross sections were 40, 5, and 13 mb, respectively. The resulting values are given in Table II together with estimated errors.

Measured charged-particle emission cross sections and spectra for each emission angle are available from the National Nuclear Data Center, Brookhaven National Laboratory, Upton, N. Y. 11973.

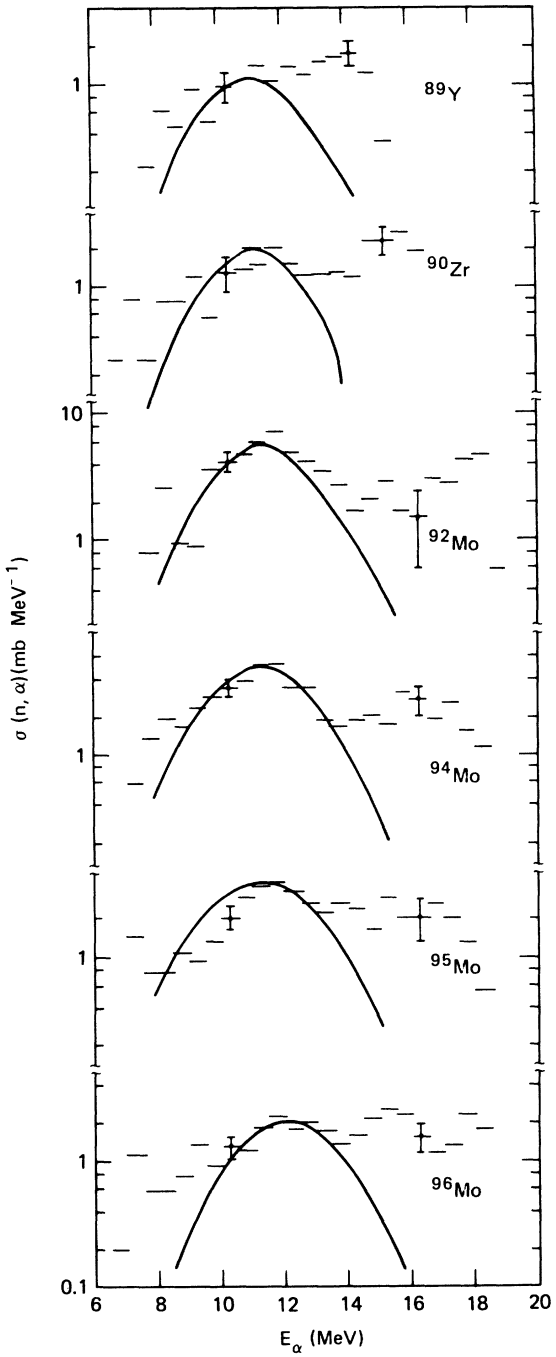

FIG. 3. Angle-integrated alpha-particle emission cross sections. The solid line denotes the results from the Hauser-Feshbach calculation.

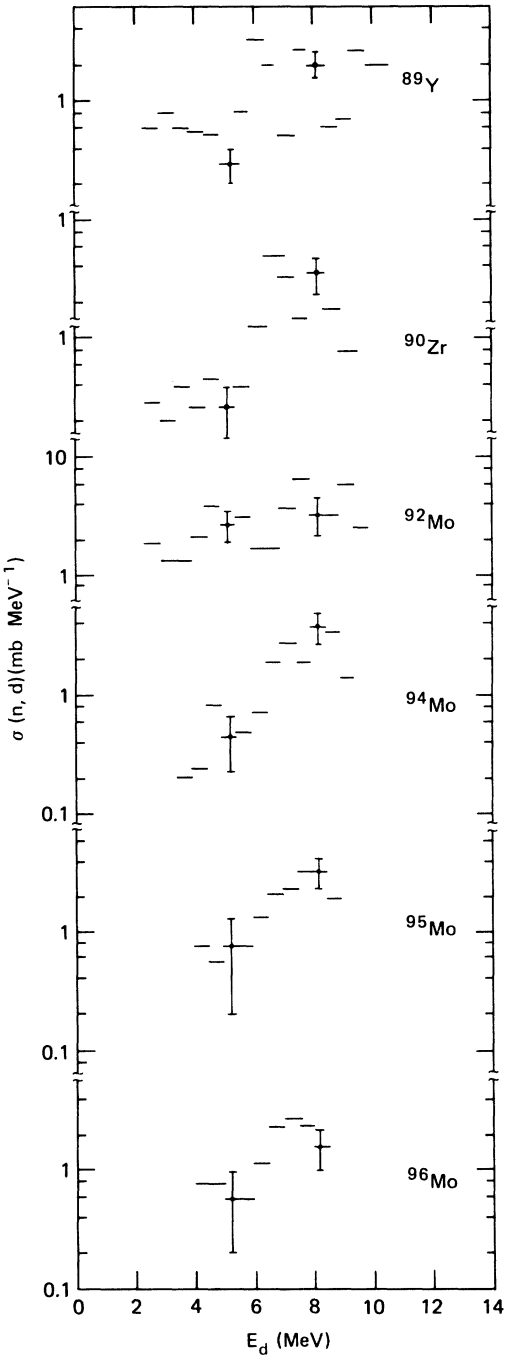

FIG. 4. Angle-integrated deuteron-emission cross sections for reactions induced by 14.8-MeV neutrons on targets of ^{89}Y, ^{90}Zr, and ^{92,94,95,96}Mo.

IV. DISCUSSION

A. General observations

The emission spectra in Figs. 2–4 and the angular distributions in Figs. 5 and 6 show that at an incident neutron energy of 14.8 MeV the proton and alpha-particle emissions proceed mainly through compound nuclear processes, whereas the deuteron emission involves usually other, probably direct, mechanisms. Similar results were obtained previously[1–3] for ^{27}Al, for isotopes in the mass region 46–63, and for ^{93}Nb. Proton spectra

TABLE II. Proton, deuteron, and alpha-particle emission cross sections and average charged-particle energies.

Target	Emission cross section (mb) protons	deuterons	alpha particles	Spectrum-averaged charged-particle energy (MeV)
^{89}Y	98 ± 12			5.8 ± 0.2
		10 ± 3		7.3 ± 0.7
			8 ± 2	12.1 ± 0.8
^{90}Zr	166 ± 20			5.5 ± 0.2
		10 ± 3		7.2 ± 1.0
			15 ± 3	12.0 ± 1.0
^{92}Mo	967 ± 116			5.2 ± 0.2
		22 ± 7		6.8 ± 0.7
			36 ± 7	13.2 ± 1.1
^{94}Mo	124 ± 15			7.4 ± 0.3
		9 ± 3		7.6 ± 0.9
			28 ± 6	12.6 ± 0.7
^{95}Mo	84 ± 10			7.7 ± 0.4
		8 ± 3		7.2 ± 0.8
			24 ± 5	13.0 ± 0.9
^{96}Mo	64 ± 8			7.6 ± 0.5
		6 ± 2		6.8 ± 1.0
			18 ± 4	13.4 ± 0.8
Mo	(195 ± 30) [a]			
		(9 ± 4) [a]		
			(20 ± 6) [a]	

[a] Inferred from isotopic data (see text).

from the proton-rich targets ^{90}Zr and ^{92}Mo show this behavior most clearly: The spectra look like multistep evaporation spectra modified by the Coulomb penetrability, and the angular distributions are isotropic for most of the proton energies.

Evidence for compound nuclear emission of deuterons is shown only for ^{92}Mo in the present data and found only for ^{27}Al in our previous measurements.[3] While the compound nucleus contribution results in a relatively large deuteron emission cross section, this cross section constitutes only a small fraction of the total emission cross section.

The spectral shapes indicate a pre-equilibrium or direct reaction mechanism for the most energetic protons and alpha particles and for most of the deuterons. Where the equilibrium contribution is small, such as for the heavier molybdenum isotopes, the pre-equilibrium component is more easily seen. As expected, this shows that the pre-equilibrium or direct component changes more slowly from isotope to isotope than the equilibrium component.

The angular distributions as represented by the ratio of Legendre-polynomial coefficients corroborate the conclusion that both pre-equilibrium and compound nuclear mechanisms are observable. The angular distributions are nearly isotropic at the peak of the evaporation spectra and become quite anisotropic at the upper ends of the spectra.

The energy at which the emission becomes anisotropic is lower than for bombardment by more energetic nucleons. In particular, for 39- and 62-MeV protons, the charged-particle emission spectra are isotropic up to energies of at least 9 MeV for proton emission and 12 MeV for alpha-particle emission[6] compared with 7 and 10 MeV, respectively, observed here. The anisotropies for the 39- and 62-MeV proton bombardment increase more slowly with outgoing particle energy as shown by the solid curves in Figs. 5 and 6. The angular distributions of protons and alpha particles of a given energy are significantly different for bombardment by 14.8-MeV neutrons from those produced by 39- and 62-MeV protons.

B. Comparison with previous data

Few data are available with which the present results can be compared. Some comparisons can be made with data on charged-particle emission, helium accumulation for (n, α) reactions, and some activation measurements.

Charged-particle emission at 14-MeV neutron energy has been measured previously only for natural zirconium and molybdenum; no isotopic

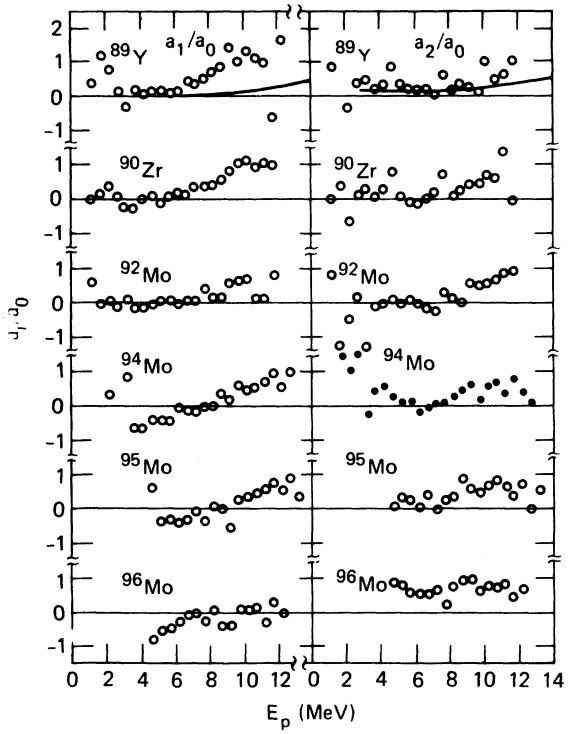

FIG. 5. Ratios of Legendre-polynomial coefficients as a function of proton-emission energy. The variation in neighboring values indicates the uncertainty of these results. At each end of the emission spectra, where the cross sections are smallest, the uncertainty is largest. The curves are for reactions induced by 39- and 62-MeV protons as given in Ref. 6.

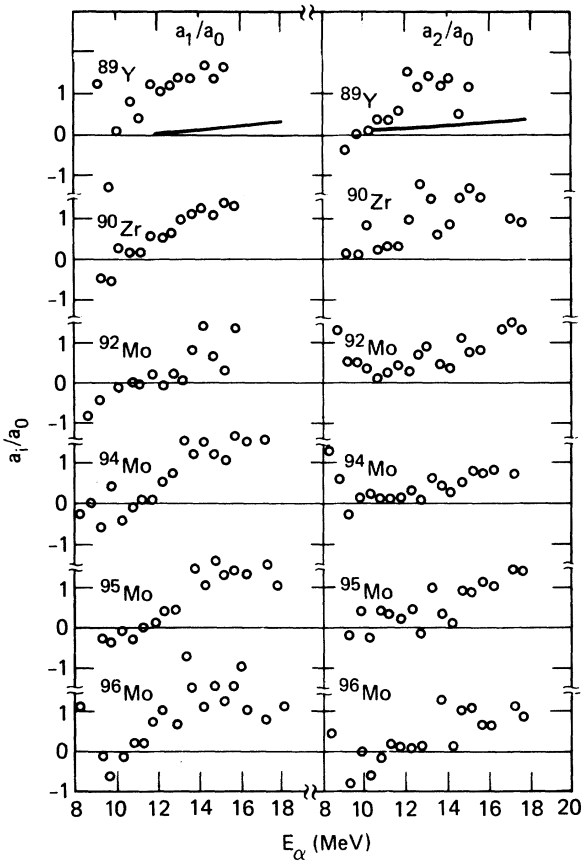

FIG. 6. Same as Fig. 5 for alpha-particle emission.

data and no measurements on yttrium have been published. The (n,p) cross section of Zr has been reported[7-9] as 180±70 mb, 62±12 mb, and 87±22 mb. Since our target ^{90}Zr constitutes only about half (51.4%) of natural zirconium, our value for $^{90}Zr(n,p)$ of 166±20 mb is not inconsistent with published values. The trend of decreasing (n,p) cross section with increasing neutron number makes it probable that the cross section for natural zirconium is less than our value for ^{90}Zr. The $Zr(n,\alpha)$ cross section of 10±10 mb given in Ref. 7 is consistent with our value of 15±3 mb for $^{90}Zr(n,\alpha)$.

The only angular distributions previously reported for $Zr(n,p)$ are in Ref. 9 for protons below 8 MeV for which the distribution around 90° was symmetric. For $Zr(n,\alpha)$ forward peaking was found[7] for alpha particles of energy greater than 6 MeV. These results are consistent with ours.

Charged-particle spectra have been reported for $Zr(n,p)$.[9] The peak around 2 MeV in the proton spectrum of Ref. 9 is not found in our $^{90}Zr(n,p)$ spectrum. The lowest energy at which we find a peak in this mass region is above 4 MeV.

For molybdenum, charged-particle emission measurements have been reported only for the (n,p) reaction.[8-10] Allan[8] reports a $Mo(n,p)$ cross section of 120±20 mb which is less than our value of 195± 30 mb. Allan obtained his result from a measurement at 120° assuming isotropic emission. Forward peaking of the distribution would raise his value by an estimated 20% and bring it into rough agreement with ours. Correcting Allan's result for protons below the threshold of detection (3 MeV in Ref. 8) and for energy loss in the target foil (of unstated thickness) would raise his value further and bring it into agreement with ours. Colli *et al.*[10] report a cross section of 143±14 mb for $Mo[(n,p)+(n,d)]$. Their value is probably low because of the large target thickness, 38 mg/cm², and the 3-MeV proton-energy cutoff. Their conclusion that the high energy end of the proton-emission spectrum is peaked forward agrees with ours.

Helium-accumulation measurements[11] for elemental molybdenum at $E_n = 14.8$ MeV yield a cross section of 15±2 mb, which agrees with our result of 20±6 mb. Our earlier results for other ele-

ments had given slightly lower values than those in Ref. 11.

Activation data can be compared with the present results only in a few cases. For several reactions the residual nucleus is stable, e.g., ^{90}Zr$(n,\alpha)^{87}$Sr, ^{94,95}Mo$(n,\alpha)^{91,92}$Zr, ^{89}Y$(n,n'p)^{88}$Sr, ^{90}Zr$(n,n'p)^{89}$Y, and ^{94}Mo$(n,n'p)^{93}$Nb. For others, the residual nuclides are long-lived and their activity has not been measured, e.g., ^{92}Mo$(n,p)^{92}$Nb$(t_{1/2}=3.2\times10^7$ yr), ^{94}Mo$(n,p)^{94}$Nb$(t_{1/2}=2\times10^4$ yr), and ^{96}Mo$(n,\alpha)^{93}$Zr$(t_{1/2}=1.5\times10^6$ yr). Of the reactions investigated here, only the following can be compared with activation data: ^{89}Y(n,α), ^{92}Mo(n,α), and ^{95,96}Mo$(n,p)^{95,96}$Nb. For these, we assume that three-body final states can be ignored.

Published values of the ^{89}Y$(n,\alpha)^{86}$Rb cross section span two orders of magnitude. Compilations based on recent measurements[12,13] give 5.5 ±1 mb and 5.5 ±0.5 mb compared with the present value of 8 ±2 mb assuming no $(n,n'\alpha)$ contribution. Our calculations, described below, predict that the $(n,n'\alpha)$ contribution is negligible. Our results are therefore consistent with the activation cross section.

The ^{92}Mo$(n,\alpha)^{89}$Zr activation cross section has been evaluated[12,13] to be 20 ±8 mb or 22 ±3 mb or somewhat less than our value of 36 ±7 mb. The activation value of Ref. 13 is based primarily on one measurement[14] that is consistent with most older less accurate values. We have found no explanation of this difference: The cross section is large enough that contaminants should not affect our experiment; there are no long-lived isomers of ^{89}Zr that could reduce the radiochemical value; and, according to our calculations, the $(n,\alpha n)$, $(n,n'\alpha)$, $(n,p\alpha)$, and $(n,\alpha p)$ cross sections are negligible.

Comparison of ^{95,96}Mo$(n,p)^{95,96}$Nb activation results with our results is difficult because of the contribution of three-body final states. The proton-emission spectra suggest that the $(n,n'p)$ component is small, but the recent activation values[13] are 31 ±4 mb for ^{95}Mo$(n,p)^{95}$Nb compared with our value of 84 ± 10 mb and, for ^{96}Mo$(n,p)^{96}$Nb, 19 ± 2 mb compared with our value of 64 ± 8 mb. The cross sections for $(n,n'p)+(n,pn)$, according to our calculations, are 28 mb for ^{95}Mo and 11 mb for ^{96}Mo, which reduce the differences significantly but not entirely. Uncertainties in input parameters for the calculations could account for the remaining differences. Because there are many long-lived isomers in this mass region, unknown isomers may contribute to the problem.

Comparisons between our measurements and radiochemical determinations of cross sections would be more reliable if measurements of activation cross sections were available for the following reactions: ^{92}Mo$(n,n\alpha+\alpha n)^{88}$Zr, ^{95}Mo$(n,np+pn+d)^{94}$Nb, and ^{96}Mo$(n,np+pn+d)^{95}$Nb.

C. Comparison with calculations

To investigate the reaction mechanisms in detail, multistage Hauser-Feshbach calculations were performed for the statistical particle emission, and the hybrid model was used to describe the precompound emission. For the Hauser-Feshbach calculations, the computer code and the prescription for determining level-density parameters have been described previously.[2,3] Transmission coefficients for neutrons and alpha particles were obtained with the optical model parameters given by Wilmore and Hodgson[15] and by Huizenga and Igo,[16] respectively. Calculations of proton transmission coefficients were initially carried out with the optical potential proposed by Becchetti and Greenlees[17]; Hauser-Feshbach calculations with these transmission coefficients are presented in the figures. To investigate how sensitive the calculated spectra are to the optical-potential parameters, we also calculated proton transmission coefficients with the optical potential of Johnson *et al.*[18] This potential has an imaginary component which is much reduced for closed-shell nuclei. For nuclei in the mass region $A \sim 90$, the absorption cross section for protons at energies below 6 MeV predicted by the potential in Ref. 18 is only about 60% of that predicted by the potential in Ref. 17. As expected, the use of the transmission coefficients from Ref. 18 caused a substantial reduction in the proton-emission cross section relative to the calculation with the potential of Ref. 17. The shape was about the same, however, and the magnitude could be restored by appropriate adjustments in the level-density parameters. Transmission coefficients were also calculated with the potentials given by Menet[19] and Perey[20]; the coefficients for the former potential are similar to those for the Becchetti and Greenlees potential, and the coefficients for the latter are closer to the values predicted by the Johnson potential. Since these values were so similar to the two sets which were used in the calculations, we did not repeat the Hauser-Feshbach calculations with the transmission coefficients based on Refs. 19 or 20. Apparently the statistical-model calculations can fit the lower energy portion of the measured energy spectra with different choices for the optical-potential parameters.

As was found in the comparisons reported in Refs. 1 and 2, the multistage Hauser-Feshbach calculations describe the low energy portion of the emission spectra well. For ^{89}Y, ^{90}Zr, and ^{92}Mo

most of the protons in the statistical model calculation are produced in $(n,n'p)$ reactions; this results in a very large low-energy peak in the spectrum, which is also observed. According to the calculations, the remaining Mo isotopes have much smaller $(n,n'p)$ cross sections, and the protons have higher energy.

Calculated $(n,n'\alpha)$ cross sections are smaller than a millibarn; this is consistent with the observed small number of alpha particles of energies below 9 MeV and agrees with the previous conclusions[1-3] that, although the $(n,n'\alpha)$ reaction for many nuclei has a lower threshold than (n,np) or $(n, 2n)$, the high Coulomb barrier prevents the $(n,n'\alpha)$ reaction from contributing significantly to the alpha-particle production cross section.

Contributions to the proton-emission cross sections from pre-equilibrium processes were calculated with the hybrid model.[21] The calculated spectra are shown in Fig. 2. Particularly for the heavier Mo isotopes, nonequilibrium reactions are responsible for a large fraction of the cross section. The calculated nonequilibrium cross section tends to be less than the observed cross section for the most energetic protons.

The deuteron and alpha-particle spectra likewise showed evidence of nonequilibrium contributions. The relative importance of nonequilibrium contributions to the alpha spectra is larger than for the targets with $A \sim 50$ to 65 examined in Ref. 1. As has been found in previous studies[1-3] of nuclei with A between 27 and 93, (n,d) reactions at 14 MeV proceed largely through nonstatistical processes.

ACKNOWLEDGMENTS

The authors would like to thank Mark S. Tillack, Joseph W. Johnson, and Steven J. Zinkle for their help in the data analysis. This work was performed under the auspices of the U. S. Department of Energy.

---

*Present address: Center for Radiation Research, National Bureau of Standards, Washington, D.C. 20234.

[1]S. M. Grimes, R. C. Haight, K. R. Alvar, H. H. Barschall and R. R. Borchers, Phys. Rev. C 19, 2127 (1979).

[2]S. M. Grimes, R. C. Haight, and J. D. Anderson, Phys. Rev. C 17, 508 (1978).

[3]S. M. Grimes, R. C. Haight, and J. D. Anderson, Nucl. Sci. Eng. 62, 187 (1977).

[4]K. R. Alvar, H. H. Barschall, R. R. Borchers, S. M. Grimes, and R. C. Haight, Nucl. Instrum. Methods 148, 303 (1978).

[5]Target foils supplied by Isotope Sales Division, Oak Ridge National Laboratory, Oak Ridge, Tennessee 37830.

[6]C. Kalbach and F. Mann Phys. Rev. C 23, 112 (1981).

[7]A. H. Armstrong and J. E. Brolley, Jr., Phys. Rev. 99, 330 (1955).

[8]D. L. Allan, Nucl. Phys. 24, 274 (1961).

[9]S. H. Ahn, J. R. Hearst, J. H. Roberts, and E. N. Strait, Phys. Rev. 119, 1667 (1960).

[10]L. Colli, U. Facchini, I. Iori, M. G. Marcazzan, and A. M. Sona, Nuovo Cimento 13, 730 (1959).

[11]H. Farrar IV and D. W. Kneff, Trans. Am. Nucl. Soc. 28, 197 (1978).

[12]M. Bormann, H. Neuert, and W. Scobel, in *Handbook on Nuclear Activation Cross-Sections* (IAEA, Vienna, 1974), pp. 87–138.

[13]S. M. Qaim, in Handbook of Spectroscopy (Chemical Rubber Company Press, Cleveland, to be published), Vol. III.

[14]S. M. Qaim, R. Wölfle, and G. Stöcklin, in *Proceedings of the International Conference on Chemical Nuclear Data, Measurements and Application, Canterbury, 1971* (Institute of Civil Engineers, London, 1971), pp. 121–128.

[15]D. Wilmore and P. E. Hodgson, Nucl. Phys. 55, 673 (1964).

[16]J. R. Huizenga and G. J. Igo, Nucl. Phys. 29, 462 (1962).

[17]F. D. Becchetti and G. W. Greenlees, Phys. Rev. 182, 1190 (1969).

[18]C. H. Johnson, A. Galonsky, and R. L. Kernell, Phys. Rev. C 20, 2052 (1979).

[19]J. J. H. Menet, E. E. Gross, J. J. Malanify, and A. Zucker, Phys. Rev. C 4, 1114 (1971).

[20]F. G. Perey, Phys. Rev. 131, 745 (1963).

[21]M. Blann, Nucl. Phys. A213, 570 (1973).